ISSN 1392–1320 MATERIALS SCIENCE (MEDŽIAGOTYRA). Vol. 20, No. 4. 2014

Methionine – Au Nanoparticle Modified Glassy Carbon Electrode: a Novel Platform for Electrochemical Detection of Hydroquinone

Jiahong HE [1, 2, 3], Zhongrong SONG [2], Shengtao ZHANG [1 *], Lin WANG [2], Ying ZHANG [2], Ri QIU [3]

[1] *School of Chemistry and Chemical Engineering, Chongqing University, Chongqing 400044, P. R. China*
[2] *School of Materials and Chemical Engineering, Chongqing University of Arts and Sciences, Yongchuan 402160, P. R. China*
[3] *Science and Technology on Marine Corrosion and Protection Laboratory, Luoyang Ship Material Research Institute, Qingdao 266101, P. R. China*

crossref http://dx.doi.org/10.5755/j01.ms.20.4.6477

Received 17 February 2014; accepted 02 October 2014

A high sensitive electrochemical sensor based on methionine/gold nanoparticles (MET/AuNPs) modified glassy carbon electrode (GCE) was fabricated for the quantitative detection of hydroquinone (HQ). The as-modified electrode was characterized by scanning electron microscopy (SEM) and X-ray diffraction (XRD) techniques. The electrochemical performance of the sensor to HQ was investigated by using cyclic and differential pulse voltammetry, which revealed its excellent electrocatalytic activity and reversibility towards HQ. The separation of anodic and cathodic peak (ΔE_p) was decreased from 471 mV to 75 mV. The anodic peak current achieved under the optimum conditions was linear with the HQ concentration ranging from 8 μM to 400 μM with the detection limit 0.12 μM (3σ). The as-fabricated sensor also showed a good selectivity towards HQ without demonstrating interference from other coexisting species. Furthermore, the sensor showed a good performance for HQ detection in environmental water, which suggests its potential practical application.

Keywords: gold nanoparticles; methionine; modified electrode; hydroquinone.

1. INTRODUCTION

Hydroquinone (HQ) is one of the isomers of dihydroxybenzene, which plays an important role in fine chemistry, such as cosmetics, pesticides and food antioxidants [1]. However, as a highly toxic and lowly degradable compound, HQ is extremely harmful to living organisms even at very low concentration [2]. For human beings, HQ can cause fatigue, headache, tachycardia and kidney damage [3]. At the high concentration, HQ will lead to acute myeloid leukemia [4]. In US and European countries, HQ is considered as a pollutant to environment [5]. In China, the national standard (GB 8978-1996) regulates that the emission concentration of phenolic compounds should be less than 0.5 mg L^{-1} (4.45×10^{-3} mol L^{-1} for dihydroxybenzene) [6]. Consequently, it is necessary to develop analytical methods with high sensitivity and accuracy to detect HQ.

Currently, different approaches, such as spectrophotometry [7], high performance liquid chromatography [8–9], capillary electrochromatography [10–11], gas chromatography [12], fluorescence quenching [13–14], electrochemiluminescence [15–16], have been proposed to determine the concentration of HQ. Nevertheless, the practical application of these methods is still restricted by many disadvantages, e. g., formidable instrumentation, lengthy analysis time and tedious process. As a conventional method, electrochemical analysis has played an important role in analytical chemistry due to the fast response, low instrument cost and feasibility for on-site measurement [17–18]. Recently, much effort has been paid to develop the versatile electrodes to determine HQ. Typical examples are the modified electrodes, and the materials to decorate the surface adopt electrospun carbon nanofibers [19], L-cysteine oxide/gold [20], poly (thionine) [21], carbon nanotube-ionic liquid composite [22], Pt-MnO_2 composite particle [23], graphitic mesoporous carbon [24], 1-butyl-3-methylimidazolium hexafluorophosphate ($BMIMPF_6$) [25], copper hexacyanoferrate and platinum film [26]. Gold nanoparticles (AuNPs), due to its large surface area, high conductivity and electrocatalytic capability, have been employed to increase the detection limit in electrochemical analysis [27]. Many studies have used AuNPs modified electrodes for voltammetric sensing [28–31], On the other hand, amino acids are cheap and popular compounds, which are easily achieved. To date, there are rare works using amino acids as modifiers to decorate the electrodes for determining the target compounds [32].

In this paper, a methionine/gold nanoparticles modified glassy carbon electrode (MET/AuNPs/GCE) was fabricated and employed as the working electrode for HQ determination. The combination of AuNPs and methionine (MET) firmly increased the electron transfer rate and the active area of the electrode. On measuring the performance of the sensor to HQ, linear range and detection limit was evaluated and discussed. The experimental results indicated that the as-modified electrode exhibited excellent electrochemical catalytic activities towards the redox of HQ.

2. EXPERIMENTAL

2.1. Reagents

Hydroquinone (HQ) was obtained from Aladdin reagents. Methionine (MET) and $HAuCl_4$ were both

*Corresponding author. Tel.: +86-23-65102531. fax: +86-23-65102531.
E-mail address: *20110901036@cqu.edu.cn* (S. Zhang)

purchased from Sigma Chemical Co. (St. Louis, MO, USA). Disodium hydrogen phosphate and dihydrogen phosphate were purchased from Nanjing Chemical Reagent Co., Ltd. All reagents used in this study were analytical grade. Doubly distilled water was employed for all the experiments.

2.2. Apparatus

A conventional three-electrode system was used for electrochemical experiments. The working electrode was a bare glassy carbon electrode (GCE) (CHI104, $d = 3$ mm) or a GCE electrode modified with MET-AuNPs composite films. A platinum wire and a saturated calomel electrode (SCE) were used as counter and reference electrode, respectively. In this manuscript, all of the potentials are reported taking SCE as the reference. Cyclic voltammetry (CV) and differential pulse voltammetry (DPV) measurements were conducted on a CHI 660D electrochemical workstation (Shanghai Chenhua Co., Ltd., China). Electrochemical impedance spectroscopy (EIS) measurements were performed on PARSTAT2273 electrochemical workstation (EG&G, USA). The surface morphology of the MET/AuNPs/GCE was characterized by a field emission scanning electron microscope (FE-SEM, Zeiss Ultra 55, Germany). Energy disperse spectroscopy (EDS) was obtained from Oxford Instruments, X-max. X-ray diffraction (XRD) was performed by a Bruker D8 Advance X-ray diffractometer with Cu Kα radiation. All the measurements were carried out at room temperature.

2.3. Preparation of MET/AuNPs/GCE

As shown in Scheme 1, the procedure for fabricating the MET/AuNPs/GCE includes three steps. In the first step, the GCE was polished using 0.05 μm alumina slurries on a polishing cloth, then washed and ultrasonicated with anhydrous alcohol and double distilled water for 5 min each and dried in N_2 atmosphere. In the second step, electrodeposition of AuNPs was performed using potentiostatic method in 1 mM $HAuCl_4$ solution containing 0.5 M H_2SO_4 at –0.2 V. The $HAuCl_4$ solution was deoxygenated for 20 min with N_2 prior to electrodeposition. In the third step, MET was electrodeposited onto AuNPs/GCE by CV technique in deoxygenated 10 mM MET solution in NaH_2PO_4–Na_2HPO_4 (PBS) for 20 cycles in the potential range of –0.8 V to 1.5 V at 100 mV s^{-1}.

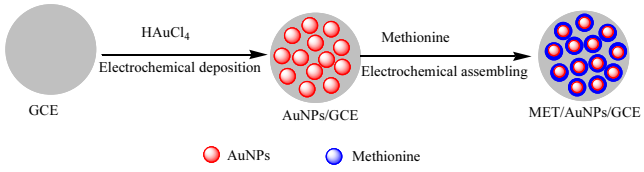

Scheme 1. The fabrication steps of the modified electrode

3. RESULTS AND DISCUSSION

3.1. SEM and XRD Characterization

SEM image (as shown in Fig. 1, a) illustrates the surface morphology of the MET/AuNPs/GCE. Plenty of MET/AuNPs composites uniformly disperse on the electrode surface. The composite has a granular shape and its average size reaches *ca.* 100 nm. The SEM image also shows that the surface of the electrode is very rough. This unique surface can increase the specific surface area of the electrode and minimize the diffusion path for ions to move in and out. We can conclude that the MET/AuNPs film provides a favorable micro-environment for electrochemical sensing the target molecules [33]. To identify the elemental composition of the MET/AuNPs modified electrode, EDS measurement was carried out. The corresponding result is shown in Fig. 1, b. The peaks appearing at 1.7, 2.1, 9.7 and 11.4 keV are related to Au, and the other peak at ~0.3 keV corresponds to C. The EDS spectrum of MET/AuNPs composite film demonstrates the presence of Au and C in the composite film, which indirectly confirms that the AuNPs and MET were successfully electrodeposited on the surface of GCE. Besides, the XRD pattern in Fig. 2 further confirms that the AuNPs are successfully anchored on GCE surface. Three peaks appearing at 44.91º, 62.44º, 77.03º are assigned to the (200), (220), (311) faces respectively, indicating the formation of the crystalline Au [25]. Meanwhile, the peaks near to 30º and 52º are corresponding to the substrate.

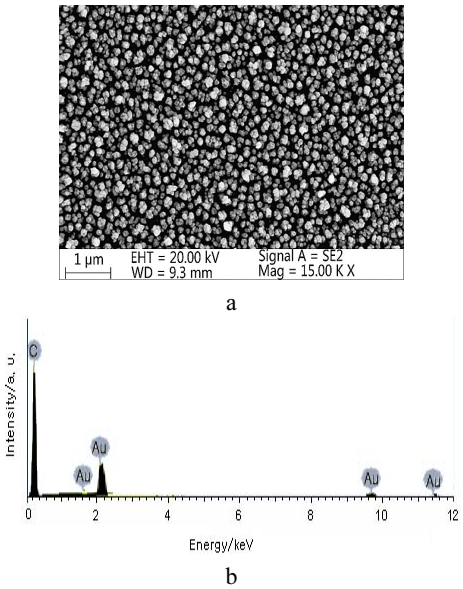

Fig. 1. SEM image (a) and EDS (b) of the MET/AuNPs/GCE

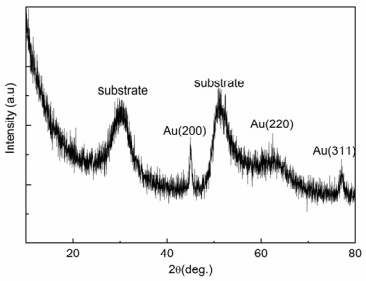

Fig. 2. XRD pattern of MET/AuNPs/GCE

3.2. Electrochemical impedance spectroscopy studies of MET/AuNPs/GCE

The EIS is employed to investigate the electron transfer property of the electrodes modified by different materials. The electrochemical impedance property of the bare GCE, AuNPs/GCE, and MET/AuNPs/GCE is respectively measured in 5.0 mM $Fe(CN)_6^{3-/4-}$ aqueous solution using 0.1 M KCl as the supporting electrolyte. In Fig. 3, EIS results show that all of the curves contain

semicircle, which corresponds to the electron-transfer process. The diameter is equal to the electron-transfer resistance (R_{et}). As shown in Fig. 3, R_{et} of AuNPs /GCE is calculated as 477.3 Ω, which is much lower than that of bare GCE (693.7 Ω), which is attributed to the acceleration effect of AuNPs for electron transfer between solution and electrode interface. In addition, the R_{et} of the MET/AuNPs/GCE was further decreased to 163 Ω, which might be the synergetic effect between MET and AuNPs.

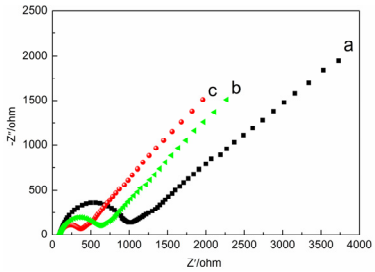

Fig. 3. Nyquist plot of the EIS for the bare GCE (a), AuNPs/GCE (b), and MET/AuNPs/GCE (c) in 5.0 mM $[Fe(CN)_6]^{3-/4-}$ solution containing 0.1 M KCl

3.3. Electrochemical behavior of HQ on electrodes

The electrochemcial response of different electrodes including GCE, AuNPs/GCE, and MET/AuNPs/GCE to HQ was studied by CV. As shown in Fig. 4, there are a couple of redox peaks appearing at 0.267 V and –0.204 V in curve a. When the GCE was modified with AuNPs, the separation of the anodic and cathodic peak potential (ΔE_p) decreases to 95 mV (curve b) and the current of the redox peaks remarkably increases, which indicates that the AuNPs can improve the electron transfer between HQ and electrode. It also illustrates that the electrochemical reversibility of HQ is improved. From the Fig. 4, c, it can be observed that the peak current at MET/AuNPs/GCE further increases. The ΔE_p for HQ becomes 75 mV. The phenomenon may be owing to the high surface area and strong adsorptive ability of MET/AuNPs film, which can effectively improve HQ accumulation on the electrode surface.

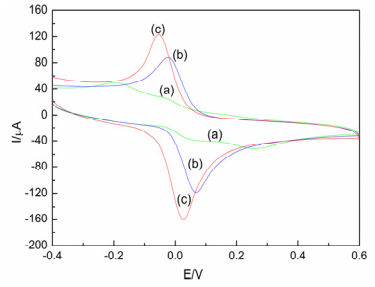

Fig. 4. Cyclic voltammograms at different electrodes in 0.1 M PBS (pH 7.0) containing 100 μM hydroquinone. GCE (a), AuNPs/GCE (b), MET/AuNPs/GCE (c). Scan rate: 100 mV s^{-1}

The excellent performance of MET/AuNPs/GCE can be assigned as the following reasons. Firstly, the amino and carboxyl in MET are able to interact with the hydroxyl group of HQ via H-bonding. In pH 7.0 PBS buffer solution, the negatively charged MET will interact with the positively charged HQ (pK_a 9.96) through the favorable electrostatic attraction, which may help to lower the activation energy of the redox reactions [20]. Secondly, as revealed by the SEM characterization, MET was decentralized and assimilated on the surface of the AuNPs having large surface area and good conductivity, which may lead to a remarkable synergistic effect for accelerating the electron transfer between HQ and MET/AuNPs/GCE. Thirdly, MET has a large surface area, which can easily enrich HQ on the surface of MET/AuNPs/GCE. Thus, MET/AuNPs/GCE has a good performance for the determination of HQ.

3.4. Effect of solution pH

The acidity of electrolyte may affect the electrochemical reaction of HQ, since protons are involved in the process of electrode reaction. In order to obtain the optimal electrochemical response of HQ at MET/AuNPs/GCE, such as PBS, acetate buffer solution (HAc-NaAc) and Britton-Robinson buffer solution (B-R) are investigated by CV tests. The results reveal that well-defined and large peak currents are obtained in PBS buffer solution. The influence of the solution pH value on the oxidation current response of HQ at MET/AuNPs/GCE is also investigated using PBS buffer solution in the pH range of 3.0 ~ 9.0. The maximum anodic peak current is observed at pH 7.0 and then decreases rapidly, which might be caused by the shortage of proton at high pH value. The peak potential (E_p) changes to more negative value with the increasing solution pH value, which indicates that protons are involved in the electrode reaction [34]. The oxidation peak potential of HQ is linear to the solution pH value with regression equation as E_p (mV) = –61.0776 pH+ + 532.8759 (R = 0.9993). The slope of curve is close to the theoretical value of –57.6 V pH^{-1}, suggesting that two protons are involved in the electrode reaction [35].

3.5.Effect of scan rate

The influence of potential scan rates on the anodic currents of HQ at the MET/AuNPs/GCE is also investigated by CV technique in 0.1M PBS (pH 7.0) containing 50 μM HQ (Fig. 5, a).

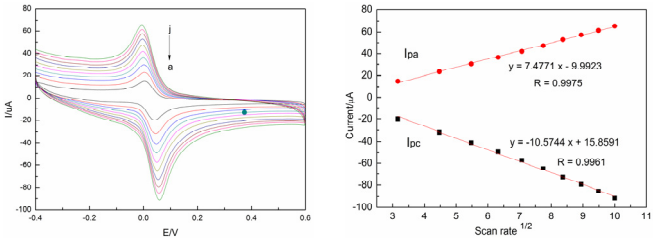

a b

Fig. 5. Effect of scan rate on the redox behavior of 50 μM HQ in pH 7.0 PBS buffer solution at MET/AuNPs/GCE at different scan rates (from a to j: 10, 20, 30, 40, 50, 60, 70, 80, 90 and 100 mV s^{-1}) – (a). The linear relationship of I_p vs. $v^{1/2}$ in the range from 10 mV s^{-1} to 100 mV s^{-1} – (b)

The result reveals that the oxidation peak current of HQ is linear to the square root of scan rate ranging from 10 to 100 mV s^{-1} (Fig. 5, b). The regression equations are expressed as I_{pa} (μA) = 7.4771 $v^{1/2}$ + 9.9923 (v: mV s^{-1}) and I_{pc} (μA) = –10.5744 $v^{1/2}$ + 15.8591 (v: mV s^{-1}), with the regression coefficient of 0.9975 and 0.9961, respectively. It also indicates that the oxidation peak

potentials of HQ do not shift positively with increasing the scan rate. The result suggests that the redox reaction of HQ is a typical diffusion-controlled process.

3.6. The response characteristics of the sensor to HQ

The amperometric responses to HQ are studied at the bare GCE, AuNPs/GCE, MET/GCE and MET/AuNPs/GCE. During these experiments, 0.025 V is set as the working potential. Under such condition, the amperometric response will reach a maximum value. The corresponding typical current-time curves are obtained by plotting the different reaction time against the anodic peak current (Fig. 6). It is observed that the sensor rapidly responds and reaches a steady state within a short time after the addition of HQ into the solution. This phenomenon could be attributed to the well-defined surface area [36]. Furthermore, drastic increase in the response currents is observed at the MET/AuNPs/GCE with the addition of the HQ (Fig. 6, curve d). Nevertheless, the bare GCE (Fig. 6, curve a), AuNPs/GCE (Fig. 6, curve b) and MET/GCE (Fig. 6, curve c) show relatively small current responses to HQ. The above results indicate that the MET/AuNPs composite films built on the GCE substrate can greatly enhance the electrocatalytic response to HQ.

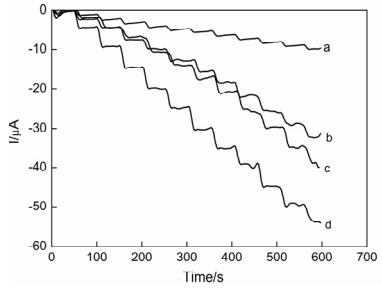

Fig. 6. Typical current-time response curves of the various electrodes to the successive additions of HQ at applied potential 25 mV: bare GCE (a); AuNPs/GCE (b), MET/GCE (c); MET/AuNPs/GCE (d)

3.7. Determination of HQ

Fig. 7, a, shows the DPV recording for various concentrations of HQ in PBS (pH 7.0). Under the optimal conditions, the oxidation peak current of HQ increases linearly to the concentration of HQ from 8 μM to 400 μM with the linear regression equation as $I_{pa} = -62.0408 - 0.4689\,c$ (μA, μM, $R = 0.9963$), and the detection limit is 0.12 μM (3σ) (Fig. 7, b).

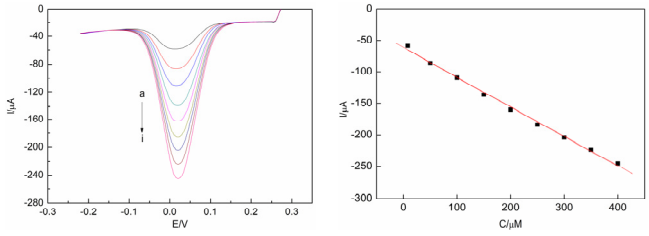

a b

Fig. 7. DPV responses (a) for various HQ concentration at MET/AuNPs/GCE in pH 7.0 PBS buffer solution. (a – i: 8, 50, 100, 150, 200, 250, 300, 350 and 400 μM). The calibration plots of HQ (b)

Compared with other previously reported modified electrodes, the MET/AuNPs/GCE displays superior electroanalytical behavior (listed in Table 1)

Table 1. Comparison of different modified electrodes for HQ determination.

Electrodes	Technique	Linear range (μM)	Detection limit (μM)	Ref.
Grapheme-chitosan/ GCE	DPV	1–300	0.75	[6]
GMC/GCE[a]	DPV	2–50	0.37	[22]
MWCNTs/MEA[b]	I-T	1–100	0.30	[37]
Pt-Gr/GCE[c]	DPV	20–150	6.00	[38]
PASA/MWNTs/GCE[d]	DPV	6.0–100	1.00	[39]
PANI/MnO_2/GCE[e]	CV	0.2–100	0.13	[40]
LDHf/GCE[f]	DPV	12–800	9.00	[41]
HRP-SiSG/AgNPs /poly(L-Arg)/CPE[g]	DPV	1–150	0.57	[42]
MET/AuNPs/GCE	DPV	8–400	0.12	This work

[a] graphitic mesoporous carbon/GCE;
[b] Multiwalled carbon nanotubes modified multielectrode array;
[c] Pt-grapheme hybrid/GCE;
[d] poly-amidosulfonic acid/multi-wall carbon nanotubes /GCE;
[e] polyaniline/MnO_2 nanofibers/GCE;
[f] Zn/Al layered double hydroxide film/GCE;
[g] Horseradish peroxidase- silica sol-gel/ silver nanoparticles/ poly(l-arginine)/CPE.

3.8. Interference of coexisting substances

In order to assess the selectivity of the as-fabricated sensor, the interference from various substances such as NaCl, KCl, NH_4Cl, $CaCl_2$, $MgSO_4$, $Zn(NO_3)_2$, $CuCl_2$, $FeBr_3$, Na_2S, $NiCl_2$, glucose, ascorbic acid, uric acid, resorcinol and catechol are examined by DPV. It is found that 500-fold Na^+, K^+, Cu^{2+}, Zn^{2+}, Mg^{2+}, NH_4^+, Ca^{2+}, Cl^-, NO_3^-, SO_4^{2-}, 100-fold Fe^{3+}, Ni^{2+}, S^{2-}, glucose, ascorbic acid, uric acid, resorcinol and 2-fold catechol will not interfere with the determination (signal change below 6 %), which indicates that this method has an excellent anti-interference ability.

3.9. Stability and reproducibility of the as-modified electrode

Under the optimized conditions, the same MET/AuNPs/GCE electrode is employed to identify 50 μM HQ for seven times by DPV technique, and the relative standard deviation (RSD) is calculated as 1.14 %. Eight MET/AuNPs/GCEs are parallel fabricated under the same conditions for determining 50 μM HQ, showing RSD as 3.64 %. The oxidation peak currents remain 92 % of their initial values after the electrode is stored at room temperature for fourteen days.

3.10. Real sample analysis

The practical application of the MET/AuNPs/GCE electrode is investigated by the measurement of HQ in different environmental samples such as local tap water, river water and lake water without any pretreatment. The recoveries are measured by adding the known concentrations of HQ to the practical water samples with the DPV method. The results are listed in Table 2. The

recoveries are 96.6 % – 101.4 %, which reveals the feasibility of this method to the determination of HQ.

Table 2. Recovery results for HQ in practical samples

Samples	Original concentr-ation of HQ (μM)	Amount of standard HQ added (μM)	Total amount of HQ Found (μM)	Reco-very (%)	RSD (%) (n = 5)
Tap water	ND[a]	50	49.4	98.8	2.84
River water	ND[a]	50	48.3	96.6	4.26
Lake water	ND[a]	50	49.6	99.2	3.82

[a] not detected.

4 CONCLUSIONS

To sum up, a novel voltammetric sensor for determination of HQ was fabricated based on AuNPs and MET composite. The research results revealed that the MET/AuNPs composite exhibited electrocatalytic activity to HQ oxidation. Due to the high effective surface area of MET and high electrode conductivity of AuNPs, low oxidation over-potential and large peak currents were observed at the MET/AuNPs/GCE. This MET/AuNPs modified electrode presented excellent catalytic activity for the electrochemical detection of HQ. Moreover, this method was successfully applied to determine HQ in environmental water samples.

Acknowledgments

This work was supported by the Foundation of National Natural Science foundation of China (Grant No. 41101223, 21372265), Natural Science Foundation of Yongchuan (Ycstc, 2013nc8001) and Foundation of Chongqing Education Commission of China (No.KJ131205; No. KJ131203).

REFERENCES

1. **Wang, J., Park, J. N., Wei, X. Y., Lee, C. W.** Room-temperature Heterogeneous Hydroxylation of Phenol with Hydrogen Peroxide Pver Fe^{2+}, Co^{2+} Ion-exchanged Naβ Zeolite *Chemical Communications* 5 2003: pp. 628 – 629. http://dx.doi.org/10.1039/b212296k
2. **Timur, S., Pazarlioğlu, N., Pilloton, R., Telefoncu, A.** Detection of Phenolic Compounds by Thick Film Sensors Based on Pseudomonas Putida *Talanta* 61 (2) 2003: pp. 87 – 93.
3. **Zhao, G. H., Li, M. F., Hu, Z. H., Li, H. X., Cao, T. C.** Electrocatalytic Redox of Hydroquinone by Two Forms of L-proline *The Journal of Molecular Catalysis A: Chemical* 255 (1 – 2) 2006: pp. 86 – 91.
4. **Gaskell, M., McLuckie, K. I. E., Farmer, P. B.** Comparison of The Mutagenic Activity of the Benzene Metabolites, Hydroquinone and Para-benzoquinone In the supF Forward Mutation Assay: A rRole For Minor DNA Adducts Formed From Hydroquinone in Benzene Mutagenicity *Fundamental and Molecular Mechanisms of Mutagenesis* 554 (1 – 2) 2004: pp. 387 – 398.
5. **Zhang, Y., Zeng, G. M., Tang, L., Huang, D. L., Jiang, X. Y., Chen, Y. N.** A Hydroquinone Biosensor Using Modified Core-shell Magnetic Nanoparticles Supported on Carbon Paste Electrode *Biosensors and Bioelectronics* 22 (9 – 10) 2007: pp. 2121 – 2126.
6. **Yin, H. S., Zhang, Q. M., Zhou, Y. L., Ma, Q., Liu, T., Zhu, L. S., Ai, S. Y.** Electrochemical Behavior of Catechol, Resorcinol and Hydroquinone at Graphene-chitosan Composite Film Modified Glassy Carbon Electrode and Their Simultaneous Determination in Water Samples *Electrochimica Acta* 56 (6) 2011: pp. 2748 – 2753.
7. **Elzanfaly, E. S., Saad, A. S., Elaleem, A. E. B. A.** Simultaneous Determination of Retinoic Acid and Hydroquinone in Skin Ointment Using Spectrophotometric Technique (Ratio Difference Method) *Saudi Pharmaceutical Journal* 20 (3) 2012: pp. 249 – 253. http://dx.doi.org/10.1016/j.jsps.2012.03.004
8. **Gao, W. H. Quigley, C. L.** Fast and Sensitive High Performance Liquid Chromatography Analysis of Cosmetic Creams for Hydroquinone, Phenol and Six Preservatives *The Journal of Chromatography A* 1218 (28) 2011: pp. 4307 – 4311. http://dx.doi.org/10.1016/j.chroma.2011.04.064
9. **Marrubini, G., Calleri, E., Coccini, T., Castoldi, A. F., Manzo, L.** Direct Analysis of Phenol, Catechol and Hydroquinone in Human Urine by Coupled-Column HPLC with Fluorimetric Detection *Chromatographia* 62 (1 – 2) 2005: pp. 25 – 31.
10. **Liu, Y. X., Chen, Y. Z., Yang, H. H., Nie, L. H., Yao, S. Z.** Cage-Like Silica Nanoparticles-functionalized Silica Hybrid Monolith for High Performance Capillary Electrochromatography Via "One-Pot" Process *The Journal of Chromatography A* 1283 (29) 2013: pp. 132 – 139. http://dx.doi.org/10.1016/j.chroma.2013.01.112
11. **Desiderio, C., Ossicini, L. G. Fanali, S.** Analysis of Hydroquinone and Some of Its Ethers by Using Capillary Electrochromatography *The Journal of Chromatography A* 887 (1 – 2) 2000: pp. 489 – 496.
12. **Judefeind, A., Rensburg, P. J. V., Langelaar, S. Plessis, J. D.** Stable Isotope Dilution Analysis of Salicylic Acid and Hydroquinone in Human Skin Samples by Gas Chromatography with Mass Spectrometric Detection *The Journal of Chromatography B* 852 (1 – 2) 2007: pp. 300 – 307.
13. **Huang, H., Xu, M., Gao, Y., Wang, G. N. Su, X. G.** Water-soluble Fluorescent Conjugated Polymer-enzyme Hybrid System for The Determination of Both Hydroquinone and Hydrogen Peroxide *Talanta* 86 2011: pp. 164 – 169.
14. **Guo, X. Q., Deng, L., Wang, J. X.** Oligonucleotide-stabilized Silver Nanoclusters as Fluorescent Probes for Sensitive Detection of Hydroquinone *RSC Advances* 3 2013: pp. 401 – 407.
15. **Yuan, D. H., Chen, S. H., Zhang, J. J., Wang, H. J., Yuan, R., Zhang, W.** An Electrochemiluminescent Sensor for Phenolic Compounds Based on the Inhibition of Peroxy Disulfate Electrochemiluminescence *Sensors and Actuators B: Chemical* 185 2013: pp. 417 – 423.
16. **Wang, X. Y., Wang, X. B., Gao, S. M., Zheng, Y., Tang, M., Chen, B. A.** A Solid-state Electrochemiluminescence Sensing Platform for Detection of Catechol Based on Novel Luminescent Composite Nanofibers *Talanta* 107 2013: pp. 127 – 132.
17. **Song, W., Zhang, L., Shi, L., Li, D. W., Li, Y., Long, Y.-T.** Simultaneous Determination of Cadmium (II), Lead (II) and Copper (II) by Using a Screen-printed Electrode Modified with Mercury Nano-droplets *Microchimica Acta* 169 (3 – 4) 2010: pp. 321 – 326.

18. **Rajabi, H. R., Roushani, M., Shamsipur, M.** Development of A Highly Selective Voltammetric Sensor for Nanomolar Detection of Mercury Ions Using Glassy Carbon Electrode Modified with A Novel Ion Imprinted Polymeric Nanobeads and Multi-wall Carbon Nanotubes *The Journal of Electroanalytcal Chemistry* 693 2013: pp. 16 – 22.
19. **Guo, Q. H., Huang, J. S., Chen, P. Q., Liu, Y., Hou, H. Q., You, T. Y.** Simultaneous Determination of Catechol and Hydroquinone Using Electrospun Carbon Nanofibers Modified Electrode *Sensors and Actuators B: Chemical* 163 (1) 2012: pp. 179 – 185.
20. **Liu, W. L., Li, C., Tang, L., Tong, A. Y., Gu, Y., Cai, R., Zhang, L., Zhang, Z. Q.** Nanopore Array Derived from L-cysteine Oxide/Gold Hybrids: Enhanced Sensing Platform for Hydroquinone and Catechol Determination *Electrochimica Acta* 88 (1) 2013: pp. 15 – 23.
21. **Ahammad, A. J. S., Rahman, M. M., Xu, G. R., Kim, S., Lee, J. J.** Highly Sensitive and Simultaneous Determination of Hydroquinone and Catechol at Poly (Thionine) Modified Glassy Carbon Electrode *Electrochimica Acta* 56 (14) 2011: pp. 5266 – 5271. http://dx.doi.org/10.1016/j.electacta.2011.03.004
22. **Bu, C. H., Liu, X. H., Zhang, Y. J., Li, L., Zhou, X. B., Lu, X. Q.** A sensor Based on the Carbon Nanotubes-ionic Liquid Composite for Simultaneous Determination of Hydroquinone and Catechol *Colloids and Surfaces B: Biointerfaces* 88 (1) 2011: pp. 292 – 296. http://dx.doi.org/10.1016/j.colsurfb.2011.07.004
23. **Unnikrishnan, B., Ru, P. L., Chen, S. M.** Electrochemically Synthesized Pt-MnO_2 Composite Particles for Simultaneous Determination of Catechol and Hydroquinone *Sensors and Actuators B: Chemical* 169 2012: pp. 235 – 242.
24. **Yuan, X. L., Yuan, D. S., Zeng, F. L., Zou, W. J., Tzorbatzoglou, F., Tsiakaras, P., Wang, Y.** Preparation of Graphitic Mesoporous Carbon for the Simultaneous Detection of Hydroquinone and Catechol *Applied Catalysis B: Environmental* 129 2013: pp. 367 – 374.
25. **Sun, X. Y., Hu, S., Li, L. F., Xiang, J., Sun, W.** Sensitive Electrochemical Detection of Hydroquinone with Carbon Ionogel Electrode Based on $BMIMPF_6$ *The Journal of Electroanalytical Chemistry* 651 (1) 2011: pp. 94 – 99. http://dx.doi.org/10.1016/j.jelechem.2010.10.019
26. **Wu, H. Y., Hu, J. C., Li, H., Li, H. X.** A Novel Photo-electrochemical Sensor for Determination of Hydroquinone Based on Copper Hexacyanoferrate and Platinum Films Modified N-silicon Electrode *Sensors and Actuators B: Chemical* 182 2013: pp. 802 – 808.
27. **Atta, N. F., Galal, A., Attia, F. M. A., Azab, S. M.** Carbon Paste Gold Nanoparticles Sensors for the Selective Determination of Dopamine in Buffered Solution *The Journal of Electrochemical Society* 157 (9) 2010: pp. 116 – 123.
28. **Renedo, O. D., Martınez, M. J. A.** Anodic Stripping Voltammetry of Antimony Using Gold Nanoparticle-modified Carbon Screen-printed Electrodes *Analytica Chimica Acta* 589 (2) 2007: pp. 255 – 260.
29. **Bernalte, E., Sánchez, C. M., Gil, E. P.** Determination of Mercury in Indoor Dust Samples by Ultrasonic Probe Microextraction and Stripping Voltammetry on Gold Nanoparticles-modified Screen-printed Electrodes *Talanta* 97 2012:pp. 187 – 192.
30. **Xu, H., Xing, S. J., Zeng, L. P., Xian, Y. Z., Shi, G. Y., Jin, L. T.** Microwave-enhanced Voltammetric Detection of Copper (II) at Gold Nanoparticles-modified Platinum Microelectrodes *The Journal of Electroanalytical Chemistry* 625 (1) 2009: pp. 53 – 59.
31. **Wang, L., Bai, J. Y., Huang, P. F., Wang, H. J., Zhang, L. Y., Zhao, Y. Q.** Self-assembly of Gold Nanoparticles for the Voltammetric Sensing of Epinephrine *Electrochemistry Communications* 8 (6) 2006: pp. 1035 – 1040.
32. **Hoffmannová, H., Fermín, D., Krtil, P.** Growth and Electrochemical Activity of the Poly-L-lysine/poly-L-glutamic Acid Thin Layer Films: An EQCM and Electrochemical Study *The Journal of Electroanalytical Chemistry* 562 (2) 2004: pp. 261 – 265. http://dx.doi.org/10.1016/j.jelechem.2003.07.037
33. **Niu, X. L., Yang, W., Wang, G. Y., Ren, J., Guo, H., Gao, J. Z.** A Novel Electrochemical Sensor of Bisphenol A Based on Stacked Grapheme Nanofibers/Gold Nanoparticles Composite Modified Glassy Carbon Electrode *Electrochimica Acta* 98 2013: pp. 167 – 175. http://dx.doi.org/10.1016/j.electacta.2013.03.064
34. **Nematollahi, D., Shayani-Jam, H., Alimoradi, M., Niroomand, S.** Electrochemical Oxidation of Acetaminophen in Aqueous Solutions: Kinetic Evaluation of Hydrolysis, Hydroxylation and Dimerization Processes *Electrochimica Acta* 54 (28) 2009: pp. 7407 – 7415. http://dx.doi.org/10.1016/j.electacta.2009.07.077
35. **Yang, J., Hu, N. F.** Direct Electron Transfer for Hemoglobin in Biomembrane-like Dimyristoyl Phosphatidylcholine Films on Pyrolytic Graphite Electrodes *Bioelectrochemistry and Bioenergetics* 48 (1) 1999: pp. 117 – 127.
36. **Yuan, D. H., Chen, S. H., Hu, F. G., Wang, C. Y., Yuan, R.** Non-enzymatic Amperometric Sensor of Catechol and Hydroquinone Using Pt-Au-organosilica@chitosan Composites Modified Electrode *Sensors and Actuators B: Chemical* 168 2012: pp. 193 – 199. http://dx.doi.org/10.1016/j.snb.2012.03.085
37. **Wu, H. Y., Hu, J. C., Li, H., Li, H. X.** A Novel Photo-electrochemical Sensor for Determination of Hydroquinone Based on Copper Hexacyanoferrate and Platinum Films Modified N-silicon Electrode *Sensors and Actuators B: Chemical* 182 2013: pp. 802 – 808.
38. **Li, J., Liu, C. Y., Cheng, C.** Electrochemical Detection of Hydroquinone by Graphene and Pt-graphene Hybrid Material Synthesized Through a Microwave-assisted Chemical Reduction Process *Electrochimica Acta* 56 (6) 2011: pp. 2712 – 2716.
39. **Zhao, D. M., Zhang, X. H., Feng, L. J., Jia, L., Wang, S. F.** Simultaneous Determination of Hydroquinone and Catechol at PASA/MWNTs Composite Film Modified Glassy Carbon Electrode *Colloids and Surface B: Biointerfaces* 74 (1) 2009: pp. 317 – 321. http://dx.doi.org/10.1016/j.colsurfb.2009.07.044
40. **Kumar, A. S., Swetha, P., Pillai, K. C.** Enzyme-less and Selective Electrochemical Sensing of Catechol and Dopamine Using Ferrocene Bound Nafion Membrane Modified Electrode *Analytical Methods* 2 (12) 2010: pp. 1962 – 1968.
41. **Li, M. G., Ni, F., Wang, Y. L., Xu, S. D., Zhang, D. D., Chen, S. H., Wang, L.** Sensitive and Facile Determination of Catechol and Hydroquinone Simultaneously Under Coexistence of Resorcinol with a Zn/Al Layered Double Hydroxide Film Modified Glassy Carbon Electrode *Electroanalysis* 21 (13) 2009: pp. 1521 – 1526.
42. **Raghu, P., Reddy, T. M., Reddaiah, K., Jaidev, L.-R., Narasimha, G.** A Novel Electrochemical Biosensor Based on Horseradish Peroxidase Immobilized on Ag-nanoparticles/poly(l-arginine) Modified Carbon Paste Electrode Toward the Determination of Pyrogallol/Hydroquinone *Enzyme and Microbial Technology* 52 (6 – 7) 2013: pp. 377 – 385.